

Extracting resonance poles from numerical scattering data: type-II Padé reconstruction

D. Sokolovski^{a,c,d}, E. Akhmatkaya^{b,c} and S.K.Sen^d

^a*Department of Physical Chemistry, University of the Basque Country, Leioa, 48940, Spain*

^b*Basque Center for Applied Mathematics (BCAM),*

Building 500, Bizkaia Technology Park E-48160, Derio, Spain

^c*IKERBASQUE, Basque Foundation for Science, E-48011 Bilbao, Spain*

^d*School of Mathematics and Physics*

Queen's University Belfast,

Belfast BT7 1NN, United Kingdom

Abstract

We present a FORTRAN 77 code for evaluation of resonance pole positions and residues of a numerical scattering matrix element in the complex energy (CE) as well as in the complex angular momentum (CAM) planes. Analytical continuation of the S -matrix element is performed by constructing a type-II Padé approximant from given physical values [Bessis *et al* (1994); Vrinceanu *et al* (2000); Sokolovski and Msezane (2004)]. The algorithm involves iterative 'preconditioning' of the numerical data by extracting its rapidly oscillating potential phase component. The code has the capability of adding non-analytical noise to the numerical data in order to select 'true' physical poles, investigate their stability and evaluate the accuracy of the reconstruction. It has an option of employing multiple-precision (MPFUN) package [Bailey (1993)] developed by D. H. Bailey wherever double precision calculations fail due to a large number of input partial wave (energies) involved. The package has been successfully tested on several models, as well as the $F + H_2 \rightarrow HF + H$, $F + HD \rightarrow HF + D$, $Cl + HCl \rightarrow ClH + Cl$ and $H + D_2 \rightarrow HD + D$ reactions. Some detailed examples are given in the text.

PACS:34.50.Lf,34.50.Pi

Keywords: Atomic and molecular collisions, resonances, S-matrix; Padé approximation; Regge-poles.

PROGRAM SUMMARY

Manuscript Title: Extracting resonance poles from numerical scattering data: type-II Padé reconstruction.

Authors: D. Sokolovski, E.Akhmatkaya and S.K.Sen

Program Title: PADE_II

Journal Reference:

Catalogue identifier:

Licensing provisions: Free software license
Programming language: FORTRAN 77
Computer: Any computer equipped with a FORTRAN 90 compiler
Operating system: UNIX, LINUX
RAM: 256 Mb
Has the code been vectorised or parallelised: no
Number of processors used: one
Supplementary material: MPFUN package, validation suite, script files, input files, readme file, Installation and User Guide
Keywords: Resonances, S-matrix; Padé approximation; Regge-poles.
PACS: 34.50.Lf,34.50.Pi
Classification: Molecular Collisions
External routines/libraries: NAG Program Library
CPC Program Library subprograms used: N/A
Nature of problem:
The package extracts the positions and residues of resonance poles from numerical scattering data supplied by the user. The data can then be used for quantitative analysis of interference patterns observed in elastic, inelastic and reactive integral and differential cross sections.
Solution method:
The *S*-matrix element is analytically continued in the complex plane of either energy or angular momentum with the help of Padé approximation of type II. Resonance (complex energy or Regge) poles are identified and their residues evaluated.
Restrictions:
None.
Unusual features:
Use of multiple precision *MPFUN* package.
Additional comments: none
Running time:
from several seconds to several minutes depending on the precision level chosen and the number of iterations performed.
References:
[1] D. Bessis, A. Haffad, and A. Z. Msezane, Phys. Rev. A., **49** (1994) 3366.
[2] D. Vrinceanu, A. Z. Msezane, D. Bessis, J. N. L. Connor and D. Sokolovski, Chem. Phys. Lett., **324**, (2000) 311.
[3] D. Sokolovski, A. Z. Msezane, Phys. Rev. A., **70** (2004) 032710.
[4] D. H. Bailey, Algorithm 719, "Multiprecision translation and execution of Fortran programs". ACM Transactions on Mathematical Software, 19(3), (1993) 288.

LONG WRITE-UP

1. Introduction

In the last fifteen years the progress in crossed beams experimental techniques has been matched by the development of state-of-the-art computer codes capable of modelling atom-diatom elastic, inelastic and reactive integral (ICS) and differential (DCS) cross-sections to a very high accuracy [1, 2, 3, 4]. Both quantities, often structured, carry a large amount of useful information about the details of the scattering mechanism which makes further detailed analysis of the scattering data highly desirable. There are, in general, two distinct types of collisions: in a *direct* collision the partners part soon after the first encounter, while in a *resonance* collision they form an intermediate complex (quasi-molecule) which then breaks up into products (reactive case) or back into reactants (elastic or inelastic case). Often a direct and several resonance processes are possible and, in accordance with the rules of quantum mechanics, interference between them gives a complicated shape to an ICS or (and) a DCS. A collision is described by a complex valued unitary scattering (S -) matrix, whose elements are the probability amplitudes for the transitions between all initial and final states of the collision partners. The dimensions of an S -matrix are equal to the number of open channels (e.g., 1×1 in the simplest case of potential scattering) and in the following we will consider one scattering element at a time, as the development of an efficient algorithm for analytical continuation of the entire matrix remains an open problem. Mathematically, a resonance is associated with a pole of an S -matrix element. There are two types of such poles, closely related to each other.

Complex energy poles. Consider a state-to-state scattering matrix element $S_{\nu' \leftarrow \nu}(E, J)$, where E is the energy, J is the total angular momentum and ν and ν' denote the set of quantum numbers describing the state of partners before and after the collision (e.g., helicity and the vibrational and rotational quantum numbers for an atom-diatom reaction). In the presence of several long-lived intermediate states (a sharp resonances) $S_{\nu' \leftarrow \nu}(E, J)$ has poles at $E = E_n(J)$, $n = 1, 2, \dots$, close to the real axis in the fourth quadrant of the complex E -plane, i.e.,

$$S_{\nu' \leftarrow \nu}(E_n, J) = \infty, \quad \text{Re}E_n > 0, \quad \text{Im}E_n < 0 \quad (1)$$

Complex angular momentum (Regge) poles. Conversely, one can fix the value of energy E and consider $S_{\nu' \leftarrow \nu}(E, J)$ as a function of the (continuous) variable J . If so, a sharp resonances would manifest themselves as poles at $J = J_n(E)$, $n = 1, 2, \dots$, close to the real axis in the first quadrant of the complex angular momentum (CAM) plane,

$$S_{\nu' \leftarrow \nu}(E, J_n) = \infty, \quad \text{Re}J_n > 0, \quad \text{Im}J_n > 0. \quad (2)$$

Far from being just a mathematical abstraction, poles of the S -matrix element provide a practical tool for a quantitative analysis of the direct and resonance contributions to both ICS and DCS. For this purpose the Regge poles are

more useful than their complex energy counterparts (for applications of Regge poles to molecular collisions see [11]-[21]). For example, an inelastic or reactive DCS is given by the square of the probability amplitude for scattering at an angle θ , $\sigma_{\nu'\leftarrow\nu}(E, \theta) = |f_{\nu'\leftarrow\nu}(E, \theta)|^2$. For zero initial and final helicities, the scattering amplitude can be written as a partial wave sum (PWS) over all physical (i.e., non-negative integer) values of J in the form

$$f_{\nu'\leftarrow\nu}(E, \theta) = (ik_\nu)^{-1} \sum_{J=0}^{\infty} (J+1/2) P_J(\cos(\theta)) S_{\nu'\leftarrow\nu}(E, J) \quad (3)$$

where $P_J(\cos(\theta))$ is the Legendre polynomial and k_ν is the initial wave vector. Similarly, the ICS at an energy E , $\sigma_{\nu'}(E)$ is given by another sum over angular momenta,

$$\sigma_{\nu'\leftarrow\nu}(E) = (\pi/k_\nu^2) \sum_{J=0}^{\infty} (2J+1) |S_{\nu'\leftarrow\nu}(E, J)|^2. \quad (4)$$

By using the Poisson sum formula [22] one can convert either sum into a sum containing integrals over the (continuous) variable J and transform the contour of integration so as to pick up the resonance contributions of the Regge poles J_n in the first quadrant of the CAM plane. The rest of the integral is usually structureless and can be attributed to the direct scattering mechanism [10]. Such a technique for analysing differential cross sections has been developed in [23]-[37]. A method for analysing integral cross sections was introduced in [38] and extended to reactive collisions in [39, 40]. Both approaches require knowing Regge pole positions J_n as well as the corresponding residues $\rho_n^{\nu'\leftarrow\nu}$,

$$\rho_n^{\nu'\leftarrow\nu}(E) = \lim_{J \rightarrow J_n} (J - J_n) S_{\nu'\leftarrow\nu}(E, J). \quad (5)$$

The purpose of this paper is to propose a simple tool for evaluation of Regge pole positions and residues from the numerical scattering data obtained in modelling realistic atomic and molecular systems. A prototype of the program described below has been successfully applied to the analysis of the $\text{Cl} + \text{HCl} \rightarrow \text{ClH} + \text{Cl}$ reaction [26, 27], the $\text{F} + \text{H}_2 \rightarrow \text{HF} + \text{H}$ reaction [28]-[32], [39, 40], the $\text{H} + \text{D}_2 \rightarrow \text{HD} + \text{D}$ reaction [33, 34], the $\text{I} + \text{HI} \rightarrow \text{IH} + \text{I}$ reaction [24, 36, 37], and the $\text{F} + \text{HD} \rightarrow \text{HF} + \text{D}$ reaction [35].

2. Type-II Padé reconstruction of a scattering matrix element

For a simple one-channel problem, one can obtain the Regge pole positions and residues directly by integrating the Schroedinger equation for complex values of J [41, 42]. This is, however, not the case when the number of open channels and, therefore, the dimension of the S -matrix is large. A typical scattering code [2, 3, 4] calculates a discrete set $S_{\nu'\leftarrow\nu}(E, J)$ for the physical values $J = 0, 1, \dots, N$, with N chosen sufficiently large for the PWS (3) and (4) to converge. Similarly, one can obtain the values $S_{\nu'\leftarrow\nu}(E^j, J)$ for a fixed integer J on an energy grid E^j , $j = 1, 2, \dots, N$, where the values of E^j can, unlike the those

of J , be chosen arbitrarily. One can, in principle, use the first set of values to obtain Regge pole positions and residues and the second to find the CE poles.

Regge poles positions and residues. If we are interested in the CAM poles of the S -matrix element at a given energy E , it is natural to seek its analytic continuation in the form of a ratio of two polynomials of J , $P(J)/Q(J)$. If successful, we can expect at least some of the complex zeroes of $Q(J)$ to coincide with the true physical poles of the problem. It is convenient to choose the orders of $P(J)$ and $Q(J)$ close to $N/2$ (see below) and require that the ratio equals the input values of the S -matrix element, $S_{\nu' \leftarrow \nu}(E, J)$, at $J = 0, 1, \dots, N$. Such a procedure is well known in the literature [43, 44] and an approximant constructed in this manner is called Padé approximant of type II. A detailed description of the algorithm, inspired by the work of Stieltjes, can be found in [43]. The method involves constructing a continued fraction whose coefficients ϕ_j , $j = 1, 2, \dots, N$ are determined by a recursive procedure. Knowing the set of ϕ_j allows one to construct the coefficients of $P(J)$ and $Q(J)$ and, from them, the poles and zeroes of the approximant. The order of $P(J)$ is $[N/2]$ and that of $Q(J)$ is $[(N-1)/2]$, where $[A]$ denotes the integer part of A . Although simple, the just described procedure gives no clue to how exactly the Padé approximation would dispose of $[(N-1)/2]$ poles available to it, for example, when there is only one true resonance Regge pole. It has been shown in Ref.[23, 24, 25] that, typically, the poles as well as zeroes fall into three different categories:

(i) *True poles and zeros* of the S -matrix element, which are stable with respect to number of input data points and amount of non-analytical noise present in the input data. True poles and the corresponding residues are the quantities of interest.

(ii) *Froissart doublets.* These are zero-poles pairs placed near the real J axis. The doublets appear as the approximant tries to reproduce non-analytical noise present in the input data [43]).

(iii) *Background (border) poles and zeros.* These form a border of a subset Ω of the CAM plane inside which the Padé approximant faithfully reproduces the analytic function specified by the input values and beyond which the approximant fails [23, 25]. The size of the Ω depends on whether the approximated function has an oscillatory components (see below) and on the amount of non-analytical noise present in the input values. Positions of the border poles and zeroes are not necessarily stable. With the increasing amount of noise, the border shrinks and becomes less well defined, as both poles and zeroes leave it to form Froissart doublets near the real axis.

Such a behaviour is shown in Fig.1 for a model system studied earlier in [23]. In order to maximise the domain of validity of an approximant, it is beneficial to remove all rapidly oscillating factors. For a heavy (semiclassical) atom-diatom system, $S_{\nu' \leftarrow \nu}(E, J)$ typically contains a rapidly oscillating factor of the form $\exp[i\phi(J)]$ where (the constant term c is unimportant, but is kept for consistency)

$$\phi(J) = J^2 + bJ + c, \quad (6)$$

often referred to as potential phase. Its origin was discussed in [23]: $d\phi(J)/dJ =$

$2aJ + b$ represents the 'deflection function', i.e., the scattering angle for a classical trajectory with a total angular momentum J . Since reaction probability decreases rapidly with J one can replace $d\phi(J)/dJ$ by a linear and $\phi(J)$ by a quadratic form, respectively. Note that the coefficients a , b , and c are not known *a priori* and must be determined iteratively (see below). A good initial guess is $b \approx \pi$ and $a \approx -\pi/N$, which corresponds to a mostly repulsive collision in which trajectories with small angular momenta (impact parameters) are scattered backwards, and those with large ones, $J \approx N$, are scattered in the forward direction. Thus a Padé approximant takes the form

$$S_{\nu' \leftarrow \nu}^{Pade}(E, J) \equiv K_N \exp[i(aJ^2 + bJ + c)] \times \frac{\prod_{i=1}^{[N/2]} (J - Z_i)}{\prod_{i=1}^{[(N-1)/2]} (J - P_i)}, \quad (7)$$

$$S_{\nu' \leftarrow \nu}^{Pade}(E, J) = S_{\nu' \leftarrow \nu}(E, J), \quad J = 0, 1, \dots, N,$$

completely specified by the sets of zeroes $\{Z_i\}$ and poles $\{P_i\}$ and the constants a, b, c and K_N . The residue at the n -th pole in Eq.(7), J_n , is explicitly given by

$$\rho^{\nu' \leftarrow \nu}_n(E) = K_N \exp[i(aP_n^2 + bP_n + c)] \times \frac{\prod_{i=1}^{[N/2]} (P_n - Z_i)}{\prod_{i \neq n}^{[(N-1)/2]} (P_n - P_i)}, \quad (8)$$

Selection of true poles. Non-analytical noise. As discussed above, not all poles $\{P_i\}$ coincide with the true physically important poles J_n of $S_{\nu' \leftarrow \nu}$ and one needs to choose among them. Important resonance poles are typically located above the real axis in the region containing the input values of the angular momentum. They are usually easily distinguished from both Froissart doublets and the border poles (see Fig. 3a). As true poles are expected to be stable with respect to a non-analytical noise, an additional test can be provided by contaminating the original data with such a noise and then selecting the poles not affected by the contamination (see Fig.3b).

Complex energy poles. Most of the above equally applies to constructing a Padé approximant on a grid of energy values E^j , $j = 1, \dots, N$ for a given physical value of the angular momentum J . Although without a clear physical meaning, a quadratic phase similar to one in Eq.(6) could still be extracted and one obtains

$$S_{\nu' \leftarrow \nu}^{Pade}(E, J) \equiv K_N \exp[i(aE^2 + bE + c)] \times \frac{\prod_{i=1}^{[N/2]} (E - Z_i)}{\prod_{i=1}^{[(N-1)/2]} (E - P_i)}, \quad (9)$$

$$S_{\nu' \leftarrow \nu}^{Pade}(E^j, J) = S_{\nu' \leftarrow \nu}(E^j, J), \quad j = 0, 1, \dots, N.$$

Again, several of the poles $\{P_i\}$ may correspond to the true CE poles of a given partial wave, while the rest would belong to the border or form Froissart doublets (Fig.5). The true poles can be selected either on physical grounds or by contaminating the data with additional noise as discussed above.

Multiple precision. Finally, when the number of input partial waves (energy points) N becomes large (~ 100), construction of a Padé approximant may require evaluation of a polynomials of orders so high that the double precision

would be insufficient. Reference [43] estimates the required accuracy of $2N$ decimal points for N input values. We found this condition to be too restrictive, and an example when multiple precision calculations are necessary will be given in the following (see Fig.6).

3. Description of the code

The *PADE_II.f* application is a sequence of 27 FORTRAN 77 files. In addition, the Multiple Precision Floating Point Computation Package (MPFUN) [46] developed by D. H. Bailey and two utility programs, the translator (*transmp90.f*) and the validating utility (*validate.f*) are supplied. All the relevant documentation and procedure specifications are provided within the program codes.

4. Using MPFUN

At the beginning of each FORTRAN 77 file to be translated to a higher precision level, the directives (i.e., special comments) are inserted in the form

```
CMP+ PRECISION LEVEL 60
CMP+ OUTPUT PRECISION 60.
```

This determines the number of digits after the decimal point to be used in a calculation. It has been found that double precision (DP) is sufficient in calculations with $\lesssim 50$ input points. The variables in the main program or in a subprogram to be converted to multiple precision (MP) by the translator program are declared by explicit MP type directives, such as:

```
CMP+ MULTIP REAL
CMP+ MULTIP COMPLEX.
```

One must also specify whether a constant in the input program will be treated as an MP quantity. This is done by appending to the constant a flag `+0`, as in the following examples:

```
1.2345678553884665E-13+0
pi=acos(-1.0+0)
zi=dpcmpl(0.+0,1.+0)
```

For a more detailed discussion of the multiple precision options we refer the reader to Ref. [46]. We note that MP is always used in the intermediate calculations and only in some parts of the program (for example, the NAG routines cannot be converted to MP). Thus the output is always given in the DP format regardless of which level of accuracy has been used in the intermediate steps.

5. Program structure of *PADE_II* (*PADE_II.f*)

The main program contains a cycle of *niter* steps, in which the potential phase (6) is iteratively removed from the input data and a new set of poles and zeroes is recalculated at each step. If one wishes to do so, the iteration cycle can be repeated *nstime* times, each time with a different random noise to check stability of the poles, as has been discussed above. Parameters *niter*, *nstime* and the magnitude of the noise are supplied by the user and defined in the input files as discussed in the following. Given below is the calling sequence of the subroutines.

```

        call open_files
666      call noise
        call precondition
777      if(imult.eq.1)then
        call dptomp
        if(iexp.eq.1) call mulexp
        call pade1_mp
        call pade2_mp
        call findzeros_polymp
        call findpoles_polymp
        else
        call pade1
        call pade2
        call findzeros_nag
        call findzeros_poly
        call findpoles_nag
        call findpoles_poly
        endif
        call smooth
        call fit
        if (icheck.le.niter) go to 777
        call spade
        call residue
        call output
        if(nscheck.le.nstime) go to 666.
```

Here we have suppressed arguments of the subprograms described in detail in the following Section.

6. Subroutine specifications

6.1. Subroutine *OPEN_FILES* (*open_files.f*)

Two input files are employed in the subroutine *OPEN_FILES*, assigning several parameters/variables with their values and the input data for which Padé reconstruction is to be performed.

Parameters listed in the input file, 'unit 1', (the name of this input file should be specified by the user, as described in Sect. 9) are as follows:

nread: number of input data points available in 'unit 1'.

niter: number of iterations required for the convergence of the calculation

shift: this shifts the input grid points and may be used to avoid exponentiation of extremely large number when evaluating the polynomials involved. For Regge poles calculations the value $nread/2$ is suggested.

jstart and **jfin**: with all input points numbered by j between 1 and N , determine a range $jstart \leq j \leq jfin$ to be used for a Padé reconstruction. This gives the user an additional flexibility. The values $jstart = 1$ and $jfin = N$ are recommended.

inv: set to '-1' and not used in the current version of the program

dxl: defines a strip $-dxl < ImJ(ImE) < dxl$ such that all poles and zeroes within the strip will be removed when calculating the potential phase of the approximant.

Parameters listed in the input file *param.pade*, 'unit 2', are as follows:

ipar: has value either '0' or '1', depending on whether S -matrix element do not require or require parity inversion, $S_{\nu' \leftarrow \nu}(E_n, J) \rightarrow \exp(i\pi J) S_{\nu' \leftarrow \nu}(E_n, J)$. Different codes calculating S -matrix elements use different conventions, and a parity change may be necessary to bring them to a single standard.

iprec: has values of either '1' or '0' depending on whether or not the input data is to be 'preconditioned' (see below) prior to the start of a calculation.

imult: has values of either '1' or '0' depending on whether a calculation is to be performed with multiple or double precision.

nstime: number of times user would like to contaminate input data with non-analytical noise. Addition of such noise (apart from those present in the numerical data) is done in the loop labelled as '666' (see section 6). 'nstime', initially assigned to '0', indicates input data is not contaminated with random noise for the first set of iterations.

nprnt: number of points used in plotting the resultant Padé approximant for real values of the argument.

fac: determines the magnitude of the noise added to the initial data. The input parameters are passed between subroutines via common statements,

`common/print/nprnt`

```

common/para/niter,shift,jstart,jfin,inv,dx1
common/par/ipar,iprec,imult,nstime,nscheck
common/nsch/fac,nread

```

The output contains $n = jfin - jstart + 1$ values of the argument, $tt(i)$, and the function, $zfk(i)$, to be used for Padé reconstruction,

output	tt(*)	DP, real	angular momentum, energy
output	zfk(*)	DP, complex	S -matrix

Here and in the following a comment (*) indicates that a variable is passed to the main program or other subroutines through a *COMMON* statement.

6.2. Subroutine *NOISE(noise.f)*

This adds random noise to the input data,

$$S(J) \rightarrow S(J) + fac \times (g_1 + ig_2) \quad (10)$$

where g_1 and g_2 are real random variables taking values between $-1/2$ and $1/2$ and the noise magnitude fac is specified by the user in the input file *param.pade*. Random numbers are generated in *zsrnd* function (*zsrnd.f*) using the *G05CAF* subroutine of NAG program library [50] designed to generate pseudo-random real numbers, distributed between $(0,1)$. The input and output are:

input	zfk	DP, complex	S -matrix element
output	zfkns	DP, complex	S -matrix with random noise added.

6.3. Subroutine *PRECOND(precond.f)*

input	tt (*)	DP, real	input grid values
input	zfkns	DP, complex	S -matrix (with random noise)
output	ts	DP, real	shifted input grid values
output	zsm	DP, complex	preconditioned S -matrix

This subroutine prepares input data according to the values of 'ipar', 'iprec' and 'shift'.

If 'ipar=1' input data is given an additional phase, $S(J) \rightarrow S(J)\exp(i\pi J)$.

If 'iprec=1' a quadratic phase $\Phi(J) = \Phi_2 J + \Phi_3 J^2$ with $\Phi_2 = \pi$ and $\Phi_3 = \pi/(2(n-1))$, is removed from the input values, $S(J) \rightarrow S(J)\exp[-i\Phi(J)]$.

If the value of 'shift' is not zero, the grid points are shifted, $ts(i)=tt(i)-shift$.

If ipar=0, iprec=0, shift=0, the input data remains unchanged.

6.4. Subroutine *DPTOMP(dtomp.f)*

This subroutine converts DP data to an MP format. We will follow the convention that if the name of a variable ends in 'mp' the variable may be converted to MP.

input	ts	DP, real	angular momentum/energy
input	zsm	DP, complex	preconditioned S -matrix
output	tsmmp	MP, real	angular momentum/energy
output	zsmmp	MP, complex	preconditioned S -matrix

If the parameter 'imult' is set to '0' in the input file *param.pade*, the calculation will be done in double precision and will not involve MP subroutines.

6.5. Subroutines *PADE1(pade1.f)*/*PADE1_MP(pade1_mp.f)*

input	ts/tsmp	DP/MP, real	shifted angular momentum, energy
input	zsm/zsmmp	DP/MP, complex	preconditioned data
output	zphi/zphimp	DP/MP, complex	coefficients of the continued fraction

Both subroutines evaluate, following the method detailed in [43], coefficients ϕ_i of continued fraction

$$F_n(t) = \phi_1 + \frac{t - ts(1)}{\phi_2 + \frac{t - ts(2)}{\phi_3 + \frac{t - ts(3)}{\dots + \frac{t - ts(n-2)}{\phi_{n-2} + \frac{t - ts(n-1)}{\phi_{n-1} + \frac{t - ts(n)}{\phi_n}}}}} \quad (11)$$

subject to the condition that at the grid points the value $F_n(t)$ coincides with the corresponding input values, $F_n[ts(i)] = zsm(i)$, $i = 1, 2, \dots, n$.

A calculation employs *PADE1_MP* for an MP calculation ('imult=1') or *PADE1* for a DP calculation ('imult=0').

6.6. Subroutines *PADE2(pade2.f)*/*PADE2_MP(pade2_mp.f)*

With $[A]$ denoting the integer part of a number A , the continued fraction $F_n(t)$ can be written as a ratio of two polynomials $P_n(t)/Q_n(t)$ of the degrees $[n/2]$ and $[(n-1)/2]$, respectively,

$$P_n(t) = \sum_{j=0}^{[n/2]} p_j t^j, \quad Q_n(t) = \sum_{j=0}^{[(n-1)/2]} q_j t^j.$$

Subroutine *PADE2/PADE2_MP* evaluates the coefficients p_j and q_j recursively, using the method detailed in [43].

input	ts/tsmp	DP/MP, real	angular momentum/energy
input	zphi/zphimp	DP/MP, complex	rational fraction
output	kp(*)	integer	degree of $P_n(t)$
output	kq(*)	integer	degree of $Q_n(t)$
output	zpn/zpnmp	DP/MP, complex	coefficients of $P_n(t)$
output	zqn/zqnmp	DP/MP, complex	coefficients of $Q_n(t)$

A calculation employs *PADE2_MP* for MP calculations ('imult=1') or *PADE2* for DP calculations ('imult=0').

6.7. Subroutines

FINDZEROS_POLY(findzeros_poly.f),
FINDZEROS_POLYMP(findzeros_polymp.f),
FINDPOLES_POLY(findpoles_poly.f),
FINDPOLES_POLYMP(findpoles_polymp.f)

These subroutines find the roots t_j^P , $j = 1, 2, \dots, [n/2]$ of the polynomial $P_n(t)$ and the roots t_j^Q , $j = 1, 2, \dots, [(n-1)/2]$ of the polynomial $Q_n(t)$,

$$P_n(t) = p_{[n/2]} \prod_{j=1}^{[n/2]} (t - t_j^P), \quad Q_n(t) = q_{[(n-1)/2]} \prod_{j=1}^{[(n-1)/2]} (t - t_j^Q). \quad (12)$$

The subroutines call internally subroutines POLYROOTS (for DP) or POLYROOTS_MP (for MP), which find roots of a complex polynomial using Weierstrass-Durand-Kerner-Dochev type algorithm [45]. Input and output for the subroutines FINDPOLES_POLY / FINDPOLES_POLYMP is as follows,

input	zqn/zqnpm	DP/MP, complex	coefficients of $Q_n(t)$
output	zppole	DP, complex	poles after each iteration
output	zplf	DP, complex	poles after final iteration
output	zplcoff	DP, complex	coefficients $Q_n(t)$ after final iteration,

and similarly for FINDZEROS_POLY / FINDZEROS_POLYMP:

input	zpn/zpnmp	DP/MP, complex	coefficients of $P_n(t)$
output	zpzzero	DP, complex	poles after each iteration
output	zzef	DP, complex	poles after final iteration
output	zzcoff	DP, complex	coefficients $P_n(t)$ after final iteration.

6.8. Subroutines

FINDZEROS_NAG (*findzeros_NAG.f*),

FINDPOLES_NAG (*findpoles_NAG.f*)

The function of these subroutines is the same as of FINDPOLES_POLY and FINDZEROS_POLY but they use a rootfinder CO2AFF from the NAG Fortan Library [51] instead of POLYROOTS. These were introduced in order to cross-check the accuracy of the roots found by POLYROOTS in a DP calculation. With no access to the source code, we have been unable to convert NAG routines to multiple precision.

6.9. Subroutine SMOOTH (*smooth.f*)

Poles and zeroes located in the vicinity of the real axis cause rapid variations of the phase of the fraction $P_n(t)/Q_n(t)$. Evaluation of the slowly changing potential phase requires removal of such zeroes and poles from the ratio. This is done in this subroutine in the following way: the user supplies a parameter dxl defining the width of a strip in the complex t -plane, $-dxl < Imt < dxl$, and contributions from all poles and zeroes within the strip are removed from the products in Eqs.(12). The argument of the remainder is calculated as

$$\phi(t) = Arg \left[\frac{\prod'_i (t - t_i^P)}{\prod'_j (t - t_j^Q)} \right] \quad (13)$$

where primes indicate products restricted by the conditions $|Imt_i^P| > dxl$ and $|Imt_j^Q| > dxl$. The inputs and outputs to this subroutine are as follows

input	ts	DP, real	shifted angular momentum or energy
input	zpzzero(*)	DP, complex	zeros after each iteration
input	zppole(*)	DP, complex	poles after each iteration
output	tphs	DP, real	points on real axis
output	phs	DP, real	the phase $\phi(t)$.

6.10. Subroutine FIT (*fit.f*)

This subroutine fits the function $\phi(t)$ evaluated in SMOOTH to a quadratic form $\tilde{\phi}(t) = afit(3)t^2 + afit(2)t + afit(1)$ and determines the values of $afit(i)$, $i = 1, 2, 3$. Fitting is done by calling the routine E02ACF from the NAG Fortran Library [52]. The inputs and outputs to this subroutine are as follows:

input	EF	DP, real	values of t
input	f	DP, real	$\phi(t)$ computed in SMOOTH
input	NDAT=3	integer	number of the coefficients
output	A(i), i=1,3	DP, real	coefficients of the quadratic form

If the number of iterations is less than the value 'niter' specified by the user in the input file *param.pade*, $icheck < niter$, the quadratic phase is removed from the input data in the main program; the calculation repeats itself until $icheck = niter$ and the program proceeds to creating output.

6.11. Subroutine SPADE (*spade.f*)

This subroutine computes the Padé approximant, its phase, and the derivative of the phase for the values of the argument between the smallest and largest values specified by the user in OPEN_FILES. The number of the values is `nprnt` as specified in the input file *param.pade*. Sum of all the phases subtracted during iterations, preconditioning and parity are returned. The normalisation factor K_N in Eqs. (7) and (9) is computed from the values ϕ 's in Eq.(11) [43], calculated in the function ZFAC (*zfac.f*) called internally from the coefficients of the continued fraction (11) [43].

The inputs and outputs to this subroutine are as follows:

input	zphi	DP, complex	set of ϕ 's in Eq.(11)
input	phi1, phi2, phi3 (*)	DP, real	preconditioning coefficients
input	xfit(i)(*)	DP, real	$xfit(i) = \sum_{all\ iterations} afit(i)$, $i=1,3$
input	zzef(*)	DP, complex	zeros after final iteration
input	zplf(*)	DP, complex	poles after final iteration
output	zst	DP, complex	values for which the approximant is evaluated
output	zspade	DP, complex	values of the approximant
output	y(*)	DP, real	phase of the approximant
output	dydx(*)	DP, real	derivative of the phase of the approximant

6.12. Subroutine RESIDUE (*residue.f*)

This subroutine computes the residues at the poles of a Padé approximant [cf. Eq.(8)]

The inputs and outputs to this subroutine are as follows:

input	phi1, phi2, phi3 (*)	DP, real	preconditioning coefficients
input	xfit(i)(*)	DP, real	$xfit(i) = \sum_{all\ iterations} afit(i)$, $i=1,3$
input	zzef(*)	DP, complex	zeros of the approximant
input	zrt	DP, complex	poles of the approximant
output	zresid	DP, complex	set of residues for the poles of the approximant

6.13. Subroutine *OUTPUT* (*output.f*)

This subroutine writes out the output files as follows. If the short print out is produced, (`Index(run_option,"full_print") = 0`), the parameters of the Padé approximant (7) or (9) are written on *out_pade* file in the following order:

- * number of zeroes (kp), number of poles (kq),
- * kp zeroes positions,
- * kq poles positions,
- * coefficients a , b and c of the quadratic phase,
- * the constant factor K_n
- * a flag which has the values 1(0) if the parity change has (has not) been applied during the calculation.

For a test calculation involving the initial data supplied with the program, (`Index(test_option,"test") /= 0`) the same data is written on the file *out_pade_test* but in a specific format chosen to avoid machine dependent differences which may occur in the last digits of the output.

Finally, if a long print out is produced (`Index(run_option,"full_print") /= 0`) additional data is written out as follows:

1. the real part and the absolute value of the original input data selected in `OPEN_FILES` are written out on ' *inputvals* ' file.

2. A grid of *nprint* equidistant points is introduced in the region containing the input values (J or E). Coordinates of the grid points and the corresponding values of the real part and the absolute value of the Padé approximant are written on *smprod* file.

3. Coordinates of the same grid points, the corresponding values of the (continuous) phase of the Padé approximant and the values of its derivative are written on the file *phdph*.

4. Real and imaginary parts of all the zeroes of the Padé approximant are written on the file ' *zeros* '

5. Real and imaginary parts of all the poles of the Padé approximant are written on the file *poles*

6. Real and imaginary parts of all the poles and the real and imaginary parts of the corresponding residues are written on the file *resids*

Upon a successful termination of a calculation a message 'NORMAL JOB TERMINATION' is printed on the screen.

7. Additional routines

7.1. Subroutine *VALIDATION* (*validation.f*)

This routine recalculates the values of the Padé approximant at the initial input points and compares them with the input values of the S -matrix element. If validation is done, the routine writes onto *job.log* after the line 'INPUT TEST' the value $\sum_{J=J_{min}}^{J_{max}} |S(E, J) - S^{Pade}(E, J)|$ or $\sum_{j=j_{min}}^{j_{max}} |S(E_j, J) - S^{Pade}(E_j, J)|$ depending on whether CAM or CE poles are obtained.

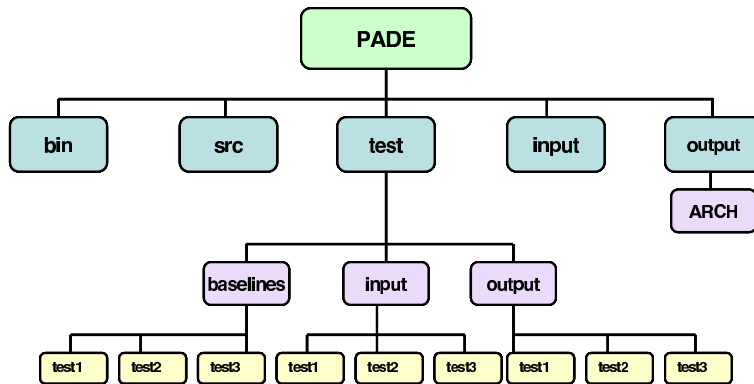


Figure 1: Schematic structure of the package

7.2. Subroutines *TRANSMP90(transmp90.f)*

This is a package of FORTRAN 77 routines developed by D.H.Bailey [46], which works in conjunction with *MPFUN*. It translates a standard FORTRAN 77 code into a code calling *MPFUN* multiple precision routines.

8. Installation

Installing and testing *PADE_II* involves unpacking the software and running the test suite.

8.1. System requirements

This version of *PADE_II* is intended for computers running the Linux/Unix operating system.

Other requirements include: FORTRAN compilers, *NAG* Numerical Libraries and a translator of FORTRAN codes to multiprecision (included in the *PADE_II* package)

8.2. Unpacking the software

The software is distributed in the form of a gzip'ed tar file which contains the *PADE_II* source code and test suite, as well as the scripts needed for running and testing the code.

To unpack the software, type the following command:

```
tar -xzvf PADE_II.tgz
```

This will create a top-level directory called *PADE* and subdirectories as shown in Fig 1. For users' benefit we supply a file *README* in directory *PADE*. The file provides a brief summary of the code structure and basic instructions for its users.

8.3. Building PADE_II executables from source

To build the executables *PADE_II* and the utilities *VALIDATE* and *TRANSMP90* (a FORTRAN -multiprecision translator) perform the following steps:

```
cd src
```

Change the definition of `F77`, `FFLAGS`, `NAGPATH` and `LFLAGS` in `Makefile` if necessary.

```
make all
```

This will create the binaries *PADE_II*, *VALIDATE*, and *TRANSMP90* in directory `PADE/bin`.

To build each executable separately simply type

```
make exe_name
```

where `exe_name` is either *PADE_II* or *VALIDATE* or *TRANSMP*.

8.4. Validation tests

The input for three jobs, *test1*, *test2* and *test3*, are provided in directories *test/input/test_name* where *test_name* is either *test1* or *test2* or *test3*. To submit and run a test suite, type the following commands:

```
cd PADE/test
```

```
./run_TEST
```

All tests are run in separate directories, *PADE/test/output/test1*, *PADE/test/output/test2* and *PADE/test/output/test3*. Each test takes about from few seconds to several minutes to run on a reasonably modern computer. To analyse the test results, inspect the message at the conclusion of the testing process. The message

```
Test test_name was successful
```

confirms that the code passed the validation test *test_name*. The results of the simulation can be viewed in the *output/test_name* directory. The message

```
Your output differs from the baseline!
```

means that the calculated data significantly differ from that in the baselines. Check the files *output/test_name/diff_file* to judge the differences.

9. Running *PADE_II*

9.1. Computational modules

PADE_II: the code for calculating the poles and zeros, as well as the poles residues in the plane of complex angular momentum / complex energy using Padé approximation of type II.

VALIDATE: the code validating the results obtained using *PADE_II*.

TRANSMP: a translation program allowing for extension of the FORTRAN 77 language to multiple precision data types.

Running *PADE_II* involves the following steps:

1. Create the input data,
2. Specify the run options and execute *PADE_II*,
3. Validate the output data (optional).

9.2. Creating input data

Two input files are required for running calculations: a parameter file, *param.pade*, and the file containing the input data to be Padé approximated. The latter can have an arbitrary name. Examples of input files can be found in directory *PADE/input*.

9.3. Executing a simulation

The script *run_PADE* in *PADE/* directory automates calculations. The following assumptions are made in the scripts:

* all binaries are placed in *PADE/bin*

* input files are located in directory *PADE/input*

* output files can be found in *PADE/output* on completion of the calculation.

Four options can be specified in the script *run_PADE* before running:

inputfile: the name of the input file. Default is *input*. The user has freedom in choosing a name for the input file

runoption: an option controlling a length of output. Please set *runoption* to *production* for a production run or to *full_print* for the detailed output (see section 6.13 for further detail). The default is *production*

testoption: an option allowing for a use of the test script *run_TEST* in *PADE/test* directory. Please set *testoption* to *test* for testing or leave blank otherwise. Default is a blank value.

validation: an option allowing for validating the output data using the utility *validate*. Please set *validation* to *valid_yes* to validate the results or to *valid_no* otherwise. The default is *valid_yes*. We encourage users to choose the default option.

We recommend running a calculation in directory *PADE/*. The command

```
../bin/run_PADE
```

immediately starts the calculation.

9.4. Output data

On completion of the calculation all output files will be redirected to *PADE/output*. The directory *ARCH* will be created automatically in *PADE/output* if it does not exist yet. Please take care of the output from the previous run in directory *PADE/output* as they will be automatically removed at the start of the next calculation. It does not apply to the content of directory *ARCH*. The following output files can be found on completion of the *PADE-II* run with the chosen *runoption* to be *production*:

out_pade contains all significant calculated data, such as zeros, poles, phase coefficients

out_pade_test contains the same data as in *out_pade* but in the different format: with 8 digits shown after the decimal point

resides contains the calculated resides

job.log contains *PADE-II* job statistics file and the summary of the validation procedure (if any)

summary.\$DATE stores the name of the input file used. *\$DATE* contains origination date and time. The file is located in *PADE/output/ARCH*.

If *runoption* is chosen to be *full_print* then a number (depending on parameters used) of output files will be created in directory *PADE/output*. Those files provide detailed information and extra control of the calculation (see 6.13).

10. Test runs

Three suitable test runs of the PADE_II program package are provided. The input and output files for these tests are included in the package.

10.1. Test 1: The hard sphere model (Regge poles)

The first test involves S matrix element for potential (single channel) scattering off a hard sphere of a radius $R-d$ surrounded by a thin semi-transparent layer of a radius R , so that the spherically symmetric potential $V(r)$ is infinite for $r < R-d$ and $\Omega\delta(r-R)$ ($\delta(x)$ is the Dirac delta) elsewhere. The energy of a non-relativistic particle is $E = k^2/2$, where we have put to unity \hbar as well as the particle's mass. A detailed discussion of this model can be found in Refs.[23] and [40]. The input file *smre.test1* contains 40 partial waves, $J = 0, 1, \dots, 39$, for a model with $d/R = 3.5/20$, $R\Omega = 50$ and $kR = 20$. The input files *param.pade* and *input_file* are as follows

```
ipar  iprec  imult  nstime  nprint  fac
0      1      0      1      2000  0.000001
```

and

```

      nread  niterr  shift  jstart  jfin  inv  dxl
      40      2      20      1      39  -1  1.5
0.0000000000000000E+000 -0.453586393436287 -0.891212311230866
1.0000000000000000      0.543023350525081  0.839717595852626
2.0000000000000000     -0.704041319711519  -0.710159010460940
3.0000000000000000      0.888058065387598  0.459731304677021
4.0000000000000000     -0.998289775531788  -5.845959347012353E-002
5.0000000000000000      0.890738274698926  -0.454516584940946
6.0000000000000000     -0.434473236117557  0.900684743457741
7.0000000000000000     -0.333662099368660  -0.942692740740534
8.0000000000000000      0.977155982861081  0.212523375558536
9.0000000000000000      0.720595526411046  0.693355671583052
10.0000000000000000     0.664031500188029  -0.747704598593613
11.0000000000000000     0.666737175185565  0.745292921760011
12.0000000000000000    -0.856249634342491  0.516562255384915
13.0000000000000000    -0.425006254859363  -0.905190412747737
14.0000000000000000     0.899356824643227  -0.437215395391851
15.0000000000000000     0.564958024126621  0.825119646460405
16.0000000000000000    -0.624574779169686  0.780965008963358
17.0000000000000000    -0.976521727561331  -0.215418930460241
18.0000000000000000    -0.404573635897627  -0.914505425427632
19.0000000000000000     0.324581052098112  -0.945857886058409
```

20.00000000000000	0.770295446722293	-0.637687168413246
21.00000000000000	0.944712675162273	-0.327899315930580
22.00000000000000	0.990708814056840	-0.136000168198755
23.00000000000000	0.998911104661369	-4.665409932903946E-002
24.00000000000000	0.999908936584357	-1.349513018612076E-002
25.00000000000000	0.999994360792535	-3.358330407996912E-003
26.00000000000000	0.99999731959201	-7.321758842783459E-004
27.00000000000000	0.99999989939087	-1.418514237449860E-004
28.00000000000000	0.99999999695326	-2.468496879744044E-005
29.00000000000000	0.9999999992432	-3.890541681219141E-006
30.00000000000000	0.99999999999844	-5.590812250283133E-007
31.00000000000000	0.99999999999997	-7.367561396623236E-008
32.00000000000000	1.00000000000000	-8.958077930733973E-009
33.00000000000000	1.00000000000000	-1.020177826822646E-009
34.00000000000000	1.00000000000000	-1.241835300295753E-010
35.00000000000000	1.00000000000000	1.384853577811148E-011
36.00000000000000	1.00000000000000	7.957477362324928E-014
37.00000000000000	1.00000000000000	1.036005717080183E-014
38.00000000000000	1.00000000000000	9.917113494880074E-015
39.00000000000000	1.00000000000000	1.000697917812276E-014

respectively. The output file *out_pade* contains the data which define a [19/19] Padé approximant (cf.Eq.7)

19 19

ZEROES

1 (39.4911990444339, 6.19497800757232)

2 (36.9799732414393, 8.43963299665421)

3 (34.0133580781357, 10.7738603477704)

4 (18.1696986797484, 18.1210578980068)

5 (12.2668387160508, 19.4124385241265)

6 (5.83305872468270, 20.3995836982532)

7 (-3.02720086016028, 20.1000359128290)

8 (24.6628733158064, 2.67477729890608)

9 (-12.0363094250139, 11.9513828909703)

10 (-12.1776119341912, 1.25316966687318)

11 (9.14176939602146, -0.234322402585798)

12 (14.5523482093869, -1.109430235203338E-003)

13 (21.8125711139416, -4.39732130205730)

14 (25.1197847383941, -10.5991913301718)

15 (26.2269224845999, -12.0435440258052)

16 (23.6585655155745, -7.73331773608408)

17 (24.6544987721333, -2.67109330547254)

18 (35.7440073905768, -3.138594025574343E-003)

19 (41.8597046798259, 3.61274050690063)

POLES

1 (35.7440073903667, -3.138542834584743E-003)

```

2 (24.6628733369383,2.67477729572751)
3 (23.6585655606588,7.73331699080323)
4 (26.2268330879602,12.0434263955026)
5 (25.1197975398861,10.5992368004622)
6 (21.8125711134792,4.39732130283915)
7 (14.5523482093869,-1.109430235909550E-003)
8 (9.14176939602135,0.234322402586938)
9 (-12.1774051901505,-1.25342226018641)
10 (-12.0359449939580,-11.9511561142494)
11 (24.6544987511749,-2.67109330818693)
12 (-3.02710863601014,-20.0995263248157)
13 (5.83307474171240,-20.3992358761048)
14 (12.2668862760970,-19.4121731020176)
15 (18.1697778070471,-18.1208548568950)
16 (34.0131260419783,-10.7739117218385)
17 (36.9796907970374,-8.43956124986996)
18 (39.4909636463193,-6.19477828169534)
19 (41.8595888739847,-3.61248175364997)
PHASE COEFF a+b*J+c*J^2
2.67555460298088      2.73887621121985      -4.727964256522786E-002
CONST FACTOR K_n
(0.357477628915536,0.933794075548949)
PARITY CHANGE FROM ORIGINAL DATA
0

```

Figure 2 shows the behaviour of the Padé approximant along the real J axis. The pole/zero configuration of the [19/19] Padé approximant is shown in Fig. 3a.

Figure 3b shows the results of two similar calculations ($nstime = 2$ chosen in the input *param.pade*). However, in each calculation a random noise with the noise factor in Eq.(10) $fac = 10^{-6}$ has been added to the input data. As discussed in Sect.2, additional contamination with a non-analytical noise results in squeezing of the domain of validity of an approximant as well as in production of additional Froissart doubles close to the real axis.

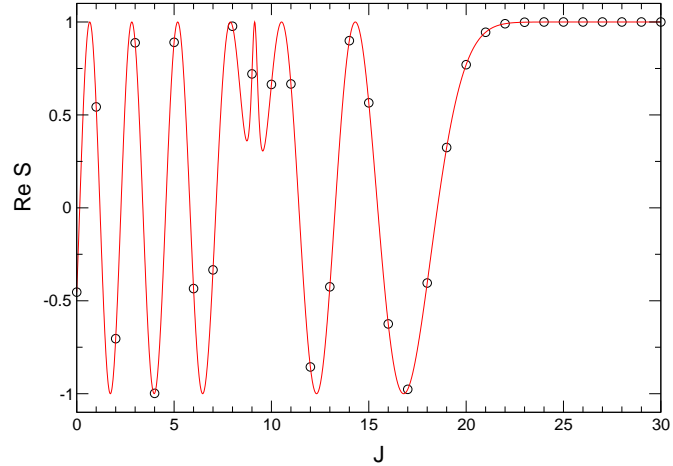


Figure 2: Real parts of the input values of the hard-sphere model matrix element $S(E, J)$, $J = 0, 1, \dots, 39$ (circles) and the real part of the $[19/19]$ Padé approximant constructed from these values (solid).

10.2. Test 2: The hard sphere model (complex energy poles)

For the second test the input file *smrj.test2* contains 49 values of $S(E, J = 10)$ on the equidistant energy grid $200 \leq R^2 E_j = R^2 k_j^2 / 2 < 250$ for the same model with $d/R = 3.5/20$, $R\Omega = 50$. The input files *param.pade* and *input.file* are as follows

```
ipar iprec imult nstime nprint fac
0 0 0 0 2000 0.000001
```

and

```
nread niter shift jstart jfin inv dxl
50 5 225. 1 49 -1 1.5
200.000000000000 0.664031500188029 -0.747704598593613
201.000000000000 0.640154019051953 -0.768246595756617
202.000000000000 0.624758751680046 -0.780817841880672
203.000000000000 0.621472411367862 -0.783436048384688
204.000000000000 0.635123092357332 -0.772410938266969
205.000000000000 0.671965187035159 -0.740582735022093
206.000000000000 0.739032006430064 -0.673670315118571
207.000000000000 0.839572088290516 -0.543248293659080
208.000000000000 0.954602056895436 -0.297884059612129
209.000000000000 0.992695675238598 0.120645332949871
```

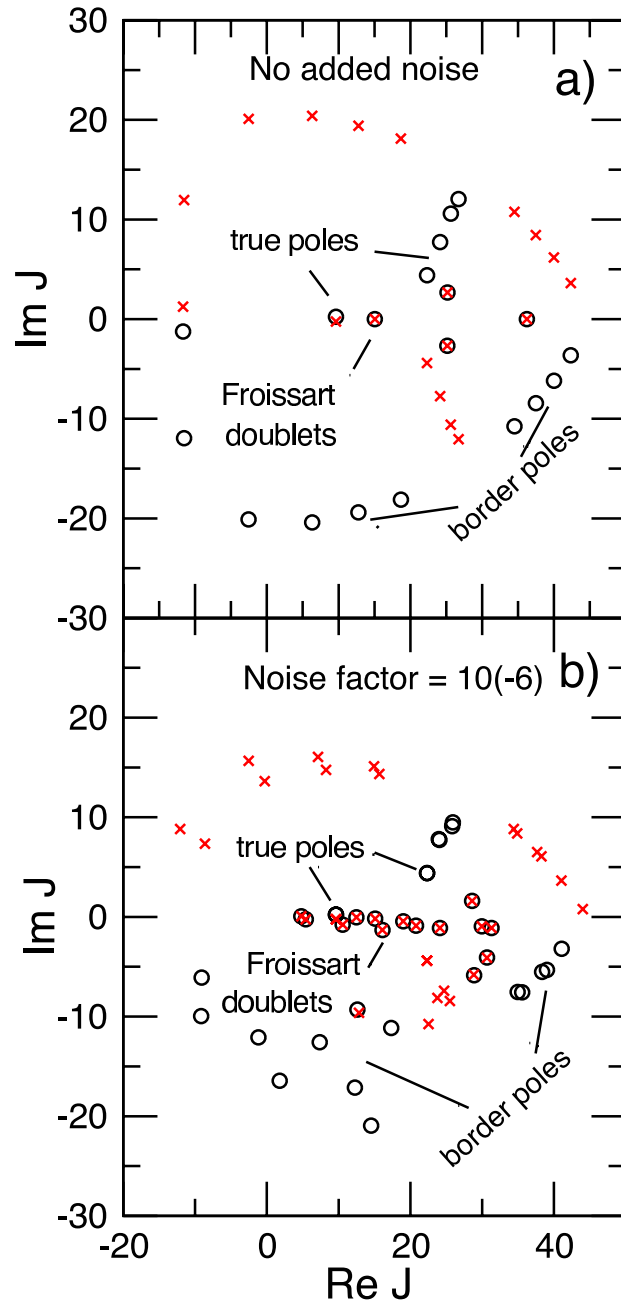


Figure 3: a) Positions of poles (circles) and zeros (crosses) in the complex angular momentum plane for the hard-sphere model. Three types of poles are indicated. The true poles include an isolated resonance with $Re J \approx 10$ on a metastable state trapped between the core and the outer layer as well as the first four poles of the infinite sequence corresponding to diffraction on the outer layer [23]. There are also several Froissart doublets. Remaining poles and zeroes mark a boundary beyond which the approximant fails, b) Poles and zeroes of two [19/19] Padé approximants constructed from the same input values, but contaminated with random noise with $fac = 10^{-6}$.

210.000000000000	0.761692689904593	0.647938458610000
211.000000000000	0.223560893654405	0.974689964464827
212.000000000000	-0.304719743630442	0.952442060096988
213.000000000000	-0.627460687663612	0.778648242428316
214.000000000000	-0.789516598726692	0.613729207660053
215.000000000000	-0.866908960431839	0.498466502709047
216.000000000000	-0.903313320122455	0.428981404829331
217.000000000000	-0.919143298112510	0.393923339667577
218.000000000000	-0.923506334424972	0.383583172567504
219.000000000000	-0.920433057855924	0.390900225129116
220.000000000000	-0.911688160524598	0.410882827530277
221.000000000000	-0.898018594051828	0.439957503330923
222.000000000000	-0.879718432979564	0.475494982808420
223.000000000000	-0.856891241732639	0.515497235532739
224.000000000000	-0.829574633076335	0.558395852560049
225.000000000000	-0.797800024420750	0.602922151719648
226.000000000000	-0.761621008213086	0.648022715534326
227.000000000000	-0.721126129965770	0.692803799556982
228.000000000000	-0.676443760254596	0.736494290006801:
229.000000000000	-0.627742897353397	0.778420744085332
230.000000000000	-0.575231856010094	0.817990410598549
231.000000000000	-0.519155855614356	0.854679587670915
232.000000000000	-0.459794039256912	0.888025586041198
233.000000000000	-0.397456205017629	0.917621144641396
234.000000000000	-0.332479399617643	0.943110517823808
235.000000000000	-0.265224455432244	0.964186697813587
236.000000000000	-0.196072515839709	0.980589398541656
237.000000000000	-0.125421575098095	0.992103537187482
238.000000000000	-5.368304983650439E-002	0.998558025434802
239.000000000000	1.872160509145225E-002	0.999824735392559
240.000000000000	9.136422532965484E-002	0.995817542690383
241.000000000000	0.163813199773938	0.986491376333227
242.000000000000	0.235636656616718	0.971841224716515
243.000000000000	0.306405561742876	0.951901061945533
244.000000000000	0.375696718367498	0.926742669681230
245.000000000000	0.443095656457025	0.896474338299161
246.000000000000	0.508199400868439	0.861239437646094
247.000000000000	0.570619106928023	0.821214853012697
248.000000000000	0.629982552997152	0.776609285882670
249.000000000000	0.685936479728164	0.727661422488601
250.000000000000	0.738148766653856	0.674637975722825
10.5000000000000	20.0000000000000	3.50000000000000
5.00000000000000	0.00000000000000E+000	

respectively. The output file *out_pade* contains the data which defines a [24/24]

Padé approximant (cf.Eq.9)

	24	24
ZEROES		
	1	(268.545717720799, 11.4671502976118)
	2	(261.728173386068, 19.6753217953572)
	3	(254.557738718419, 26.5701017472017)
	4	(245.881831513906, 33.4912944344641)
	5	(232.951306941574, 1.877662435186347E-004)
	6	(224.121052772429, 4.19191611872841)
	7	(220.411919658935, 1.15434928347258)
	8	(217.652385494978, 2.852399491808721E-002)
	9	(210.331899212664, 2.72550066138290)
	10	(209.654815139940, 2.641960499678558E-004)
	11	(212.868385932177, 3.598159766224907E-004)
	12	(186.524319063303, -9.14781503752908)
	13	(206.326496566314, 1.959778648327130E-004)
	14	(192.395056901391, -15.3604166393560)
	15	(198.447273067597, -20.3445869086093)
	16	(205.051304571580, -24.9792759962048)
	17	(212.514236963499, -29.6992072722432)
	18	(221.649194114141, -34.9881538867756)
	19	(220.510303177377, -1.14210693606552)
	20	(224.031598890991, -4.30241298271368)
	21	(226.023976865667, 2.261727493434314E-002)
	22	(238.490995343524, -1.47246931619824)
	23	(242.730754962705, -3.477317333857598E-004)
	24	(238.491169699397, 1.46793956930393)
POLES		
	1	(242.730754962705, -3.477317319122845E-004)
	2	(238.491169699401, 1.46793956929681)
	3	(226.023976865667, 2.261727493435679E-002)
	4	(224.121052772959, 4.19191611897241)
	5	(220.411919658902, 1.15434928347629)
	6	(221.648098623382, 34.9885968283023)
	7	(212.513501359997, 29.7001476182166)
	8	(205.051076178872, 24.9802350950195)
	9	(198.447298402548, 20.3453065442821)
	10	(192.395118933229, 15.3609323651784)
	11	(206.326496566310, 1.959780792806160E-004)
	12	(186.524346342521, 9.14822455412355)
	13	(212.868385932166, 3.598159852993832E-004)
	14	(209.654815139977, 2.641956005816340E-004)
	15	(210.331899212667, -2.72550066136285)
	16	(217.652385494976, 2.852399491882152E-002)
	17	(220.510303177407, -1.14210693605598)

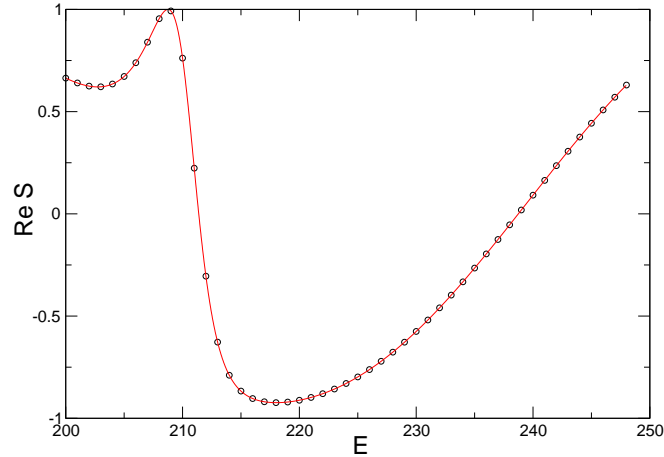


Figure 4: Real parts of $S(E_m, J = 10)$, $m = 1, \dots, 49$ (circles) and the $[24/24]$ Padé approximant constructed from these values (solid).

```

18 (224.031598890383, -4.30241298239934)
19 (232.951306941574, 1.877662434131332E-004)
20 (245.882621687043, -33.4918893250634)
21 (254.558185226003, -26.5708559777491)
22 (261.728380822961, -19.6760176672578)
23 (268.545803872059, -11.4677538269500)
24 (238.490995343520, -1.47246931620535)
PHASE COEFF a+b*J+c*J^2
-283.165777224028      2.47637834572351      -5.407538683988272E-003
CONST FACTOR K_n
(0.908740385440017, 0.417744816017221)
PARITY CHANGE FROM ORIGINAL DATA
0

```

Figure 4 shows the behaviour of the Padé approximant along the real E -axis. The pole/zero configuration of the $[24/24]$ Padé approximant is shown in Fig. 5.

10.3. Test 3: Multiple precision (Regge poles)

The third test, whose purpose is to illustrate the use of the multiple precision option, involves constructing a Padé approximant for the inelastic matrix element for the $He^+ - Ne$ inelastic collision model of Olson and Smith [53]

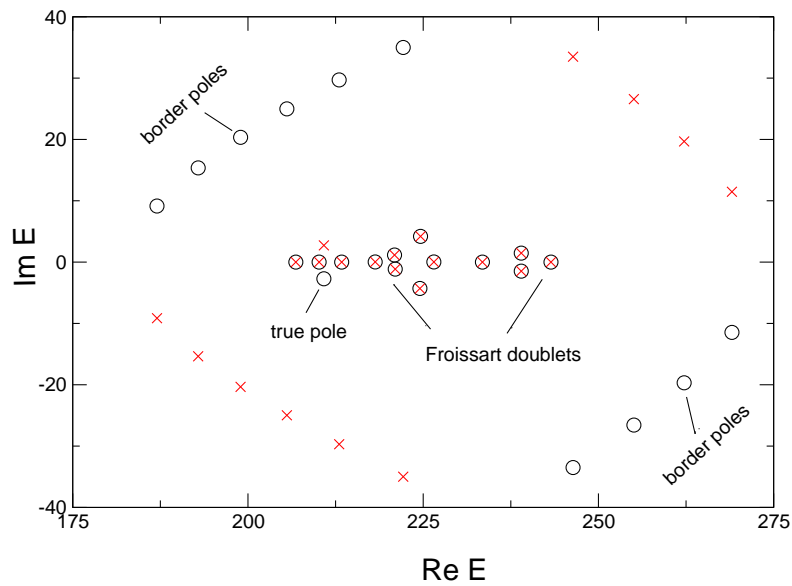


Figure 5: Positions of poles (circles) and zeros (crosses) in the complex energy plane for 10-th partial wave ($J = 10$) of the hard-sphere model. Three types of poles are indicated. The true pole with $ReE \approx 212$ corresponds to a metastable state trapped between the core and the outer layer. There are also several Froissart doublets. Remaining poles and zeroes mark a boundary beyond which the approximant fails.

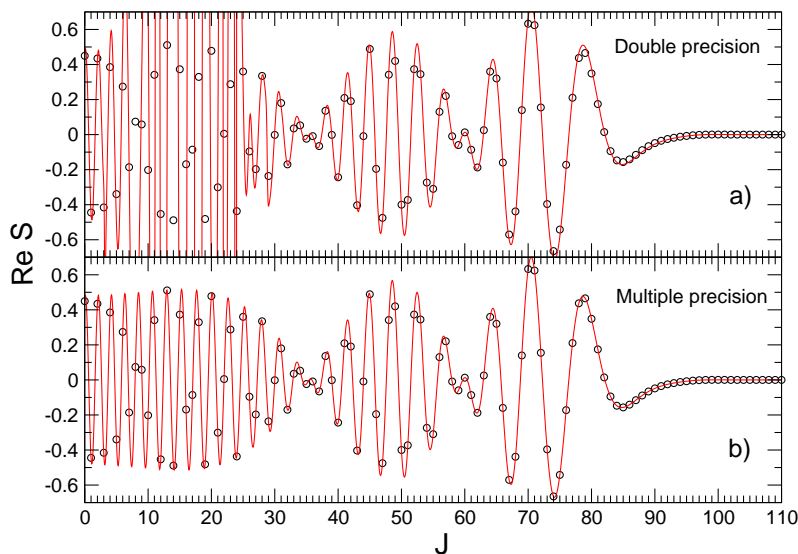


Figure 6: Real parts of $S(E_m, J = 10)$, $m = 1, \dots, 49$ (circles) and the $[55/55]$ Padé approximant constructed from these values (solid).

computed by K.Thylwe [54]. The input consists of 111 partial waves, i.e., the values of $S_{01}(E, J)$, $J = 0, 1, \dots, 110$ at a fixed value of the collision energy. The input file *param.pade* is

```

ipar iprec imult nstime nprint fac
0 1 1 0 2000 0.000001

```

and the input *input_file* together with the output *out_pade*, too long to be printed here, are supplied with the code. The number of input data is such that a double precision calculation (choosing 'imult'= 0 in *param.pade*) produces incorrect Padé approximant which fails to reproduce the input values (Fig.6a). A calculation with a multiple precision of 60 digits yields the correct approximant (Fig.6b). In general, it is recommended to repeat a DP calculation with a choice of a higher precision, in order to see if this changes the computed approximant in any significant way.

Acknowledgement

This work was supported by the U.K. EPSRC through a grant GR/S03799/01 to CCP6 (Collaborative Computational Project No. 6 on Molecular Quantum

Dynamics) for which this was the Flagship Project. DS is grateful to Daniel Bessis for useful discussions.

References

- [1] S. A. Harich, D. X. Dai, C. C. Wang, X. Yang, S. D. Chao and R. T. Skodje, Forward scattering due to slow-down of the intermediate in the $\text{H}+\text{HD}\leftarrow\text{D}+\text{H}_2$ reaction, *Nature*, **419**, (2002) 281.
- [2] D. C. Clary, Quantum Theory of Reaction Dynamics, *Science*, **279** (1998) 1879.
- [3] D. Skouteris, D. E. Manolopoulos, W. Bian, H-J Werner, L-H Lai and K. Liu, Van der Waals Interactions in the $\text{Cl} + \text{HD}$ Reaction, *Science*, **286** (1999) 1713.
- [4] P. Casavecchia, N Balucani and G. G. Volpi, Cross beam studies of reaction dynamics, *Ann. Rev. Phys. Chem.*, **50** (1999) 347.
- [5] W. H. Miller, *Adv. Chem. Phys.*, Classical-Limit Quantum Mechanics and the Theory of Molecular Collisions, **25** 69 (1974) 69.
- [6] D. Skouteris, J. F. Castillo and D. E. Manolopoulos, ABC: a quantum reactive scattering problem, *Comp. Phys. Commun*, **133** (2000) 128.
- [7] S. C. Althorpe, F. Fernández-Alonso, B. D. Bean, J. D. Ayers, A. E. Pomerantz, R. N. Zare and E. Wrede, Observation and interpretation of a time-delayed mechanism in hydrogen exchange reaction, *Nature*, **416** (2002) 67.
- [8] V. Aquilanti, S. Cavalli and D. De Fazio, Hyperquantization algorithm. I. Theory for triatomic systems, *J. Chem. Phys.*, **109** (1998) 3792.
- [9] V. Aquilanti, S. Cavalli, D. De Fazio, A. Volpi, A. Aguilar, X. Giménez and J. F. Lucas, Exact reaction dynamics by the hyperquantization algorithm: integral and differential cross sections for $\text{F} + \text{H}_2$, including long-range and spin-orbit effects, *Phys. Chem. Chem. Phys.*, **4**, 401 (2002).
- [10] It is worth noting that the applications usually require the knowledge of only a few leading true pole positions and residues. The remaining poles and zeroes of the approximant are then used to reproduce the direct part of the S -matrix element on the real axis, which is independent of their individual positions and residues.
- [11] J.N.L. Connor, Molecular collisions and the semiclassical approximation, Meldola Medal Lecture, *Chemical Society Reviews*, **5**, (1976), 125.
- [12] J.N.L. Connor, W. Jakubetz and C.V. Sukumar, Exact quantum and semiclassical calculation of the positions and residues of Regge poles for interatomic potentials, *J. Phys. B*, **9**, (1976), 1783.

- [13] J.N.L. Connor and W. Jakubetz, Rainbow scattering in atomic collisions: A Regge pole analysis, *Mol. Phys.*, **35**, (1978) 949.
- [14] J.N.L. Connor, D.C. Mackay and C.V. Sukumar, Quantum and semiclassical calculation of Regge pole positions and residues for complex optical potentials, *J. Phys. B*, **12**, (1979), L5151.
- [15] J.N.L. Connor, Semiclassical theory of elastic scattering, in "Semiclassical methods in molecular scattering and spectroscopy." Proceedings of the NATO Advanced Study Institute held in Cambridge, England, in September, 1979. Edited by M.S. Child. Reidel, Dordrecht, The Netherlands, (1980) 45.
- [16] J.N.L. Connor, D. Farrelly and D.C. Mackay, Complex angular momentum analysis of diffraction scattering in atomic collisions, *J. Chem. Phys.*, **74**, (1981) 3278.
- [17] K-E. Thylwe and J.N.L. Connor, A complex angular momentum theory of modified Coulomb scattering, *J. Phys. A*, **18**, (1985), 2957.
- [18] J.N.L. Connor, D.C. Mackay and K-E. Thylwe, Computational study and complex angular momentum analysis of elastic scattering for complex optical potentials, *J. Chem. Phys.*, **85**, (1986) 6368.
- [19] J.N.L. Connor and K-E. Thylwe, Theory of large angle elastic differential cross sections for complex optical potentials: Semiclassical calculations using partial waves, l-windows, saddles and poles, *J. Chem. Phys.*, **86**, (1987) 188.
- [20] J.N.L. Connor, New theoretical methods for molecular collisions: The complex angular momentum approach, *J. Chem. Soc., Faraday Transactions*, **86**, (1990) 1627.
- [21] P. McCabe, J.N.L. Connor and K-E. Thylwe, Complex angular momentum theory of molecular collisions: New phase rules for rotationally inelastic diffraction scattering in atom homonuclear-molecule collisions, *J. Chem. Phys.*, **98**, (1993) 2947.
- [22] D.M. Brink, *Semi-classical Methods in Nucleus-Nucleus Scattering*, Cambridge University Press, Cambridge, 1985.
- [23] D. Sokolovski and A. Z. Msezane, Semiclassical complex angular momentum theory and Padé reconstruction for resonances, rainbows, and reaction thresholds, *Phys. Rev. A.*, **70** (2004) 032710.
- [24] D. Vrinceanu, A. Z. Msezane, D. Bessis, J. N. L. Connor and D. Sokolovski, *Chem. Phys. Lett.*, Padé reconstruction of Regge poles from scattering matrix data for chemical reactions, **324** (2000) 311.

- [25] D. Sokolovski, S. Sen, On the type II Padé reconstruction of a scattering matrix element, *Semiclassical and other Methods for Understanding Molecular Collisions and Chemical reactions*, Collaborative Computational Project on Molecular Quantum Dynamics (CCP6), Daresbury, UK, (2005) 104.
- [26] D. Sokolovski, J. N. L. Connor and G. C. Schatz, New uniform semiclassical theory of resonance angular scattering for reactive molecular collisions, *Chem. Phys. Lett.*, **238** (1995) 127.
- [27] D. Sokolovski, J. N. L. Connor and G. C. Schatz, Complex angular momentum analysis of resonance scattering in the $\text{Cl} + \text{HCl} \rightarrow \text{ClH} + \text{Cl}$ reaction, *J. Chem. Phys.*, **103** (1995) 5979.
- [28] D. Sokolovski, J. F. Castillo and C. Tully, Semiclassical angular scattering in the $\text{F} + \text{H}_2 \rightarrow \text{HF} + \text{H}$ reaction: Regge pole analysis using the Padé approximation, *Chem. Phys. Lett.*, **313** (1999) 225.
- [29] D. Sokolovski, J. F. Castillo, Differential cross sections and Regge trajectories for the $\text{F} + \text{H}_2 \rightarrow \text{HF} + \text{H}$ reaction, **2** (2000) 507.
- [30] D. Sokolovski, S.K.Sen, V.Aquilanti, S.Cavalli and D.De Fazio, Interacting resonances in the $\text{F} + \text{H}_2$ reaction revisited: Complex terms, Riemann surfaces, and angular distributions *J. Chem. Phys.*, **126** (2007) 084305.
- [31] D. Sokolovski, D.De Fazio, S.Cavalli and V.Aquilanti, Overlapping resonances and Regge oscillations in the state-to-state integral cross sections of the $\text{F} + \text{H}_2$ reaction, *J. Chem. Phys.*, **126** (2007) 12110.
- [32] D. Sokolovski, D.De Fazio, S.Cavalli and V.Aquilanti, On the origin of the forward peak and backward oscillations in the the $\text{F} + \text{H}_2(v=0) \rightarrow \text{HF}(v'=2) + \text{H}$ reaction, *Phys.Chem.Chem.Phys.*, **9** (2007) 1.
- [33] F. J. Aoiz, L. Bañares, J. F. Castillo and D. Sokolovski, Energy dependence of forward scattering in the differential cross section of the $\text{H} + \text{D}_2 \rightarrow \text{HD}(v' = 3, j' = 0) + \text{D}$ reaction, *J. Chem. Phys.*, **117** (2002) 2546.
- [34] D. Sokolovski, Glory and thresholds effects in $\text{H} + \text{D}_2$ reactive angular scattering, *Chem. Phys. Lett.*, **370** (2003) 805.
- [35] D. Sokolovski, Complex-angular-momentum analysis of atom-diatom angular scattering: Zeros and poles of the S matrix, *Phys. Rev. A.*, **62** (2000) 024702-01.
- [36] D. Sokolovski, A.Z. Msezane, Z. Felfli, S.Yu. Ovchinnikov and J.H. Macek, What can one do with Regge poles?, *Nuclear Instruments and Methods in Physics Research Section B: Beam Interactions with Materials and Atoms*, Volume **261**, (2007)133.

- [37] A.J. Totenhofer, C. Noli and J.N.L. Connor, Dynamics of the $I + HI \rightarrow IH + I$ reaction: Application of nearside-farside, local angular momentum and resummation theories using the Fuller and Hatchell decompositions, *Physical Chemistry Chemical Physics*, **12**,(2010), in print.
- [38] J. H. Macek, P. S. Krstic, and S. Yu. Ovchinnikov, Regge Oscillations in Integral Cross Sections for Proton Impact on Atomic Hydrogen, *Phys. Rev. Lett.* **93**, (2004) 183203.
- [39] D. Sokolovski, D.De Fazio, S.Cavalli and V.Aquilanti, Overlapping resonances and Regge oscillations in the state-to-state integral cross sections of the $F + H_2$ reaction, *J. Chem. Phys.*, **126** (2007) 121101.
- [40] D. Sokolovski, Complex-angular-momentum (CAM) route to reactive scattering resonances: from a simple model to the $F + H_2 \rightarrow HF + H$ reaction , *Phys. Scr.*, **78** (2008) 058118.
- [41] P. G. Burke and C. Tate, A program for calculating Regge trajectories in potential scattering, *Comput. Phys. Commun.* **1**, 1969, 97.
- [42] D. Sokolovski, Z. Felffi, S. Yu. Ovchinnikov, J. H. Macek, and A. Z. Msezane, Regge oscillations in electron-atom elastic cross sections, *Phys. Rev. A* **76**,(2007) 012705.
- [43] D. Bessis, A. Haffad, and A. Z. Msezane, Momentum-transfer dispersion relations for electron-atom cross sections, *Phys. Rev. A.*, **49** (1994) 3366.
- [44] G. A. Baker, Jr., *The essentials of Padé Approximations*, Academic, New York, 1975.
- [45] M.S. Petkovic, C.Carstensen. and M. Trajkovic, Weierstrass formula and zero-finding methods, *Numerische Mathematik*, **69**: (1995).
- [46] D. H. Bailey, Algorithm 719, "Multiprecision translation and execution of Fortran programs". *ACM Transactions on Mathematical Software*, 19(3):288 (1993).
- [47] S. Sokolovski, J. N. L. Connor, Semoclassical nearside-farside theory for inelastic and reactive atom-diatom collisions, *Chem. Phys. Lett.*, **305** (1999) 238.
- [48] W. Gautschi, in *Handbook of Mathematical Functions*, edited by M. Abramowitz and I. A. Stegun (Harri Deutsch, Htun, 1984).
- [49] J. N. L. Connor, *J. Chem. Soc. Faraday Trans.*, **305** (1990) 1627.
- [50] Numerical Algorithms Group, Fortran Library Manual, Mark 19, subroutine G05CAF (NAG, OXFORD, 2002).
- [51] Numerical Algorithms Group, Fortran Library Manual, Mark 21, subroutine C02AFF (NAG, OXFORD, 2004).

- [52] Numerical Algorithms Group, Fortran Library Manual, Mark 21, subroutine E02ACF (NAG, OXFORD, 2004).
- [53] R.E. Olson and F.T.Smith Phys. Rev. A. **3**, (1971) 1607; Erratum, Phys. Rev. A. **6**, (1972) 526.
- [54] K.-E. Thylwe (to be published).